

Field-induced magnetic transition in the heavy-fermion antiferromagnet Ce₇Ni₃K. Umeo,* Y. Echizen, M. H. Jung,[†] and T. Takabatake*Department of Quantum Matter, ADSM, Hiroshima University, Higashi-Hiroshima 739-8530, Japan*

T. Sakakibara

Institute for Solid State Physics, University of Tokyo, Kashiwa, Chiba 277-8581, Japan

T. Terashima and C. Terakura

National Institute for Materials Science, Tsukuba, Ibaraki 305-0003, Japan

C. Pfleiderer, M. Uhlarz, and H. v. Löhneysen

Physikalisches Institut, Universität Karlsruhe, D-76128 Karlsruhe, Germany

(Received 14 November 2002; published 10 April 2003)

We present a detailed study of the field (B) - temperature (T) phase diagram of the heavy-fermion antiferromagnet Ce₇Ni₃ that crystallizes in the hexagonal Th₇Fe₃-type structure with three nonequivalent Ce sites (Ce_I, Ce_{II}, and Ce_{III}). This compound undergoes two magnetic transitions at $T_{N1} = 1.9$ K and $T_{N2} = 0.7$ K in zero field. Below T_{N1} , an incommensurate spin density wave (SDW) develops, and below T_{N2} a commensurate SDW appears independently. By applying fields along the c axis, both T_{N1} and T_{N2} are suppressed and vanish at 0.3 T. For $B||c > 0.7$ T, however, another magnetic phase appears below 0.5 K, which was found by magnetoresistance, specific heat, and magnetization measurements. The separation of the field induced phase from the SDW phase is attributed to large spin fluctuations of Ce_{III}, which originate from a geometrical frustration in the quasiregular tetrahedron made of Ce_I and Ce_{III}.

DOI: 10.1103/PhysRevB.67.144408

PACS number(s): 75.25.+z, 72.15.Qm, 75.30.Kz

I. INTRODUCTION

The interesting physics provided by geometrically frustrated systems is under active discussion. The geometrical frustration can occur in triangular, kagome, f.c.c. and pyrochlore lattices where nearest-neighbor interactions compete. The frustration in insulating materials leads to multiple phase transitions and novel field-induced magnetic phases.¹ When the frustration affects an itinerant magnet, unusual physical properties have been observed; spin-liquid behavior in Y_{0.97}Sc_{0.03}Mn₂ (C15 cubic Laves phase),² heavy-fermion behavior in LiV₂O₄ (spinel),³ and superconductivity in Cd₂Re₂O₇ (pyrochlore).⁴ However, there have been few studies on geometrically frustrated cerium (Ce) compounds. In CePdAl with the quasikagome lattice of Ce atoms, one-third of Ce ions remain paramagnetic in the antiferromagnetically ordered state below $T_N = 2.7$ K.^{5,6}

Another candidate for the frustrated Ce compound is Ce₇Ni₃, which crystallizes in the hexagonal Th₇Fe₃-type structure having three nonequivalent Ce sites; 1Ce_I, 3Ce_{II}, and 3Ce_{III}.⁷ As shown in the inset of Fig. 1, the Ce_I and Ce_{III} atoms form a quasiregular tetrahedron. These tetrahedra are stacked in chains along the c axis, which resemble the frustrated arrangement of Mn atoms in RMn₂ (R =rare earth) crystallizing in the hexagonal C14 Laves structure.⁸ Ce₇Ni₃ undergoes two magnetic transitions at $T_{N1} = 1.9$ K and $T_{N2} = 0.7$ K.⁹⁻¹¹ A neutron-diffraction study showed that the magnetic structure below T_{N1} is a spin-density wave (SDW) with a modulation vector $k = 0.22c^*$. The ordered moments are estimated to be $0.46 \mu_B$, $0.70 \mu_B$, and $0.10 \mu_B$ for Ce_I, Ce_{II}, and Ce_{III}, respectively.¹¹ As temperature is decreased below T_{N2} , a commensurate SDW

structure having modulation vector $k = 0.25c^*$ appears independently of the incommensurate SDW for $T_{N2} < T < T_{N1}$. The magnetic easy axis for both Ce_I and Ce_{II} is parallel to the c axis, while that for Ce_{III} is perpendicular to the c axis.¹¹

The magnetically ordered state of Ce₇Ni₃ is very sensitive to pressure and magnetic field. With application of pressure, both T_{N1} and T_{N2} decrease and vanish at $P_c = 0.39$ GPa, and non-Fermi liquid behavior appears while it might be complicated (no specific heat divided by temperature $C/T \propto -\ln T$ for $T \rightarrow 0$) in this system.¹²⁻¹⁴ This observation suggests that even at $P = 0$, the Kondo interaction competes with the Ruderman-Kittel-Kasuya-Yoshida interaction. Upon applying a rather weak magnetic field of 0.2 T along the c axis, the easy magnetization axis, the SDW state collapses, and a field-induced ferromagnetic state is stabilized.¹¹ The specific-heat measurements under magnetic fields were performed by two groups using polycrystalline samples.^{15,16} Sereni *et al.*¹⁵ showed that a field of 6 T completely smears out the magnetic ordering, while Kim *et al.*¹⁶ showed that the T_{N1} remains even at 6 T. Contradictory observations may be attributed to the effect of magnetic anisotropy. In order to study the unusual ground state of Ce₇Ni₃ under magnetic fields, we have measured the field and temperature dependences of the specific heat C , magnetization M and electrical resistivity ρ for a single crystalline sample. A field-induced magnetic (FIM) phase was found below 0.5 K when the field was applied along the c axis. In this paper, we present the B - T phase diagram and discuss the origin of the FIM phase.

II. EXPERIMENTAL PROCEDURE

For the single-crystal growth of Ce₇Ni₃, we used starting materials of Ce and Ni with a purity of 99.999%. A single

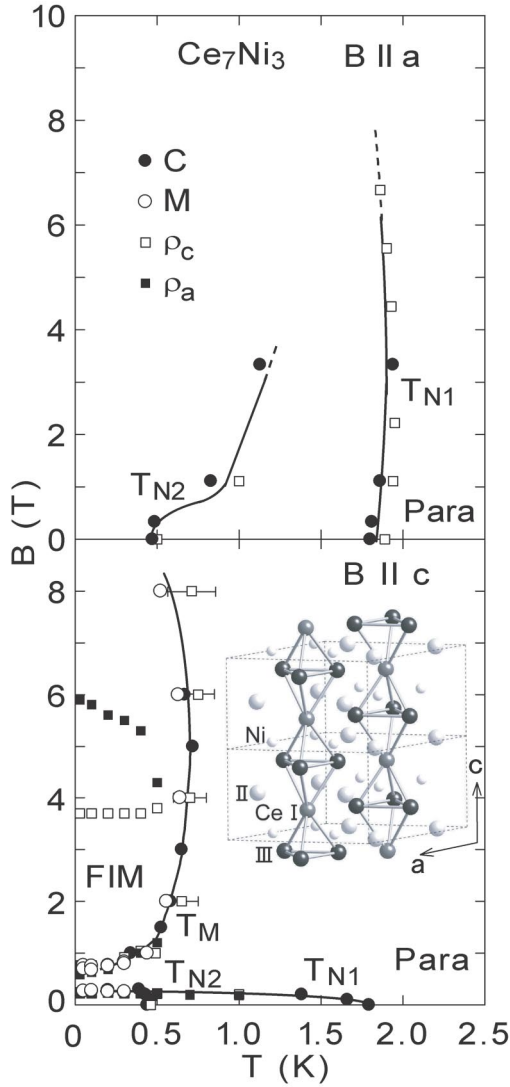


FIG. 1. Field-temperature phase diagram of Ce_7Ni_3 for $B\parallel a$ and $B\parallel c$. The solid lines are a guide to the eye. The inset shows the schematic drawing of the crystal structure of Ce_7Ni_3 . One Ce_I and three Ce_{III} atoms form a quasiregular tetrahedron, which stacks along the c axis.

crystal was grown by a Czochralsky pulling method using a radio-frequency induction furnace with a hot tungsten crucible. In order to decrease defects, strains, and impurity ions, the as-grown crystal was treated by the technique of the solid-state electrotransport. The crystal rod was self-heated to a temperature at 400°C . During this treatment for two weeks, the vacuum was better than 3×10^{-8} Pa. The crystal orientation was determined by the back-scattering Laue method. The electrical resistivity and Hall resistivity were measured by an ac four-terminal method in magnetic fields applied by a superconducting solenoid. The magnetization measurements in the temperature range $0.05 \leq T \leq 1.3$ K were performed by a Faraday method using a high-resolution capacitive magnetometer.¹⁷ The specific heat was measured by an ac method in the ranges $0.3 \leq T \leq 3$ K and $0 \leq B \leq 6$ T. The absolute value of the specific heat was determined using the value measured by an adiabatic heat-pulse

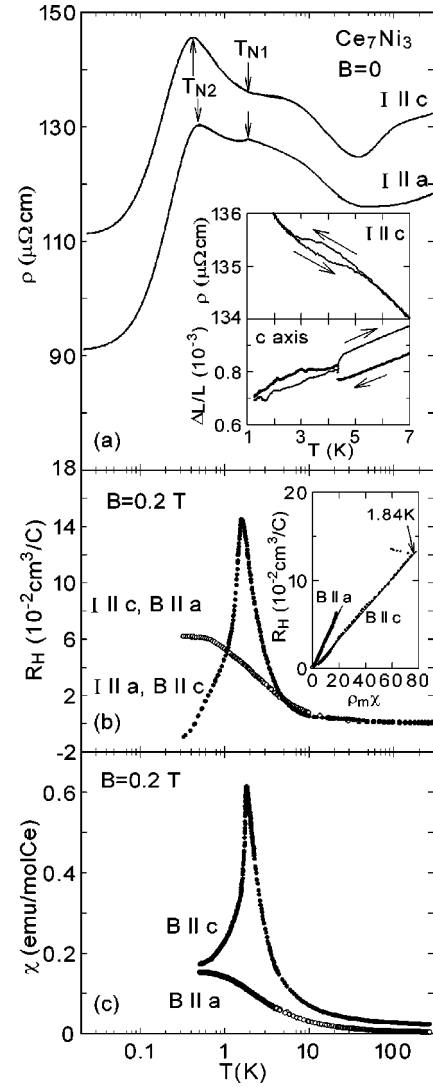


FIG. 2. Temperature dependence of the electrical resistivity $\rho(T)$ for the current directions $I\parallel a$ and $I\parallel c$, Hall coefficient $R_H(T)$ for the two configurations of electrical current I and applied magnetic field B , and magnetic susceptibility $\chi(T)$ for $B\parallel a$ and $B\parallel c$ of Ce_7Ni_3 . The inset of (a) shows the resistivity and thermal expansion along the c axis at low temperature. The inset of (b) shows the R_H against $\rho_m \chi$, where ρ_m is the magnetic part of the resistivity and χ is the magnetic susceptibility (see text).

method.¹⁰ The thermal expansion was measured using a strain gauge method.

III. RESULTS AND DISCUSSION

Before presenting the detailed experimental results, we summarize the magnetic field (B)-temperature (T) phase diagrams of Ce_7Ni_3 for $B\parallel a$ and $B\parallel c$ in Fig. 1. The diagrams emphasize the highly anisotropic behavior of T_{N1} . For $B\parallel a$ up to 6 T, T_{N1} remains at about 1.9 K and T_{N2} increases with fields, while for $B\parallel c$ both T_{N1} and T_{N2} vanish at 0.3 T. Upon increasing $B\parallel c$ above 0.7 T, a FIM phase appears. Because this phase is separated from the SDW phase present below 0.3 T, it is unlikely to be a spin-flop phase in a conventional

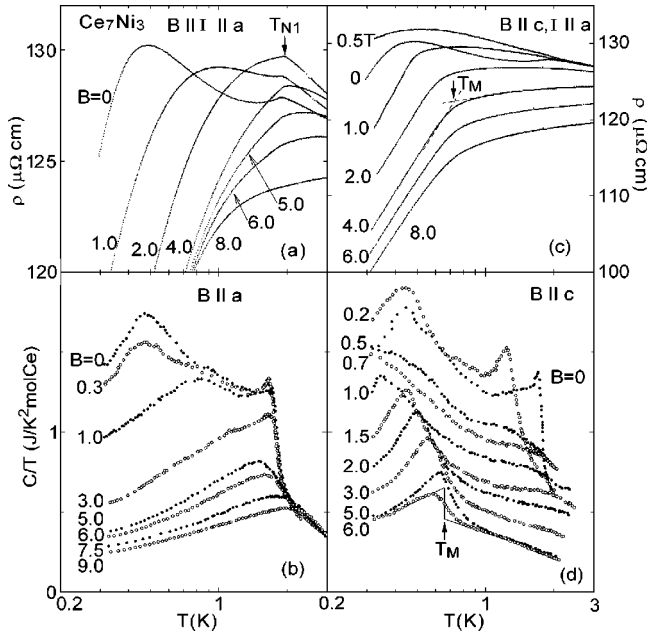


FIG. 3. Temperature dependence of electrical resistivity $\rho(T)$ for the current direction $I\parallel a$ and specific heat divided by temperature C/T of Ce_7Ni_3 under magnetic fields for $B\parallel a$ and $B\parallel c$. T_M was taken as the cross point of the two lines as depicted in (c), and the temperature of the inflection point of C/T in (d).

antiferromagnet. Instead, the FIM phase appearing from a paramagnetic phase is analogous to the field-induced antiferromagnetic phase reported for the frustrated insulating compound $\text{Gd}_3\text{Ga}_5\text{O}_{12}$.¹⁸

Now, we present the electrical resistivity $\rho_a(T)$ and $\rho_c(T)$ along the a and c axis of Ce_7Ni_3 in zero field in Fig. 2(a). The significant increases of $\rho_a(T)$ and $\rho_c(T)$ below 40 K are due to the Kondo effect. As shown in the inset, there exists a small hysteresis in $\rho_c(T)$ around 4 K, where the thermal expansion along the c axis exhibits a distinct jump. These observations suggest a lattice distortion along the c axis at around 4 K. The neutron diffraction study¹¹ indicated that the symmetry of the space group at 1.4 K is lowered to $P3m1$, in which the screw operation in $P6_3mc$ is lost. Therefore, the distortion along the c axis may result from the structural transition into a lower symmetry phase.

With decreasing temperature below $T_{N1}=1.9$ K, $\rho_c(T)$ increases steadily. Such an increase of resistivity at the SDW transition temperature for certain Ce compounds is explained by the superzone-gap formation on the Fermi surface along the propagation vector of SDW's. If gap formation reduces the carrier number, then the absolute value of the ordinary Hall coefficient R_0 should increase. The Hall coefficient R_H is given by the sum of R_0 and the anomalous Hall coefficient R_a . The latter arises from magnetic scattering (skew scattering) and is expressed as $R_a = D\rho_m\chi$, where D , ρ_m , and χ are a constant factor, the magnetic contribution to $\rho(T)$ from $4f$ electrons, and the magnetic susceptibility, respectively. For Ce_7Ni_3 , the $R_H(T)$ for $B\parallel c$ has a sharp peak at $T_{N1}=1.8$ K as shown in Fig. 2(b), which is identical to that of $\chi(T)$ for $B\parallel c$ as shown in Fig. 2(c). This fact suggests that the SDW gap on the Fermi surface is very small and/or imperfect, and

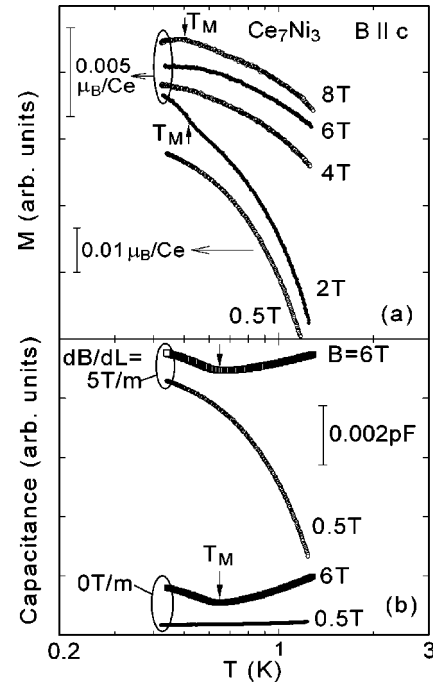


FIG. 4. Temperature dependence of magnetization (a) and capacitance of the magnetometer under magnetic fields for $B\parallel c$. T_M was taken as the temperature of a kink in the $M(T)$ and minimum of the capacitance.

the main part of R_H originates from R_a . As shown in the inset of Fig. 2(b), the R_H above T_{N1} is almost linear against $\rho_m\chi$. For both $B\parallel a$ and $B\parallel c$, the value of R_0 obtained by the linear extrapolation to $\rho_m\chi=0$ is $0.2 \times 10^{-3} \text{ cm}^3/\text{C}$, which is close to those of heavy fermion metals, such as CeAl_2 ($0.33 \times 10^{-3} \text{ cm}^3/\text{C}$) and CeCu_2Si_2 ($0.26 \times 10^{-3} \text{ cm}^3/\text{C}$).¹⁹

The increases of $\rho_a(T)$ at $T_{N2} < T < T_{N1}$ can not be explained by the effect of SDW's with $k\parallel c$, but may be attributed to spin fluctuations along the a axis. $\rho_a(T)$ and $\rho_c(T)$ pass through pronounced maxima at T_{N2} and reach the large residual values of 90 and 110 $\mu\Omega \text{ cm}$, respectively. It should be noted that the large residual resistivity does not originate from lattice defects or impurities, but from the remaining spin fluctuations. This argument is based on the fact that both ρ_a and ρ_c are largely suppressed by magnetic field, as shown in Figs. 3 and 6.

In the following, we will discuss the magnetic phase diagram in more detail. Figure 3 shows the low-temperature data of resistivity $\rho(T)$ and specific heat divided by temperature C/T at various constant fields, $B\parallel a$ and $B\parallel c$. For $B\parallel a$, the peaks in both $\rho_a(T)$ and C/T at T_{N1} remain up to 6 T, and the maxima at T_{N2} shift to higher temperatures. On the other hand, the peaks in both $\rho_a(T)$ and C/T at T_{N1} vanish for $B\parallel c \geq 0.5$ T. At 0.5 T, a short-range magnetic order manifests itself in a broad maximum in $\rho_a(T)$ and a broad shoulder in C/T at 0.6 K. At 0.5 and 0.7 T, the continuous increase of C/T on cooling strongly suggests that spin fluctuations remain at low temperatures. Above $B\parallel c = 1$ T, a sudden decrease of $\rho_a(T)$ and another peak in C/T appear at around 0.5 K, which suggest the FIM transition. By integrating the

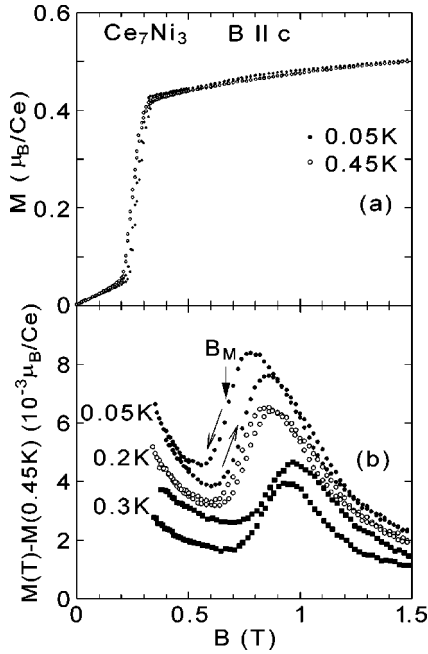


FIG. 5. Field ($B\parallel c$) dependence of magnetization of Ce_7Ni_3 at 0.45 and 0.05 K (a), and difference $\Delta M = M(T) - M(0.45 \text{ K})$ for $T = 0.05, 0.2$, and 0.3 K (b). The field-induced magnetic transition field B_M was taken as the field of the inflection point of $\Delta M(B)$.

C/T data at 2 T, we estimate the entropy released at the FIM transition temperature T_M to be $0.53 \text{ J/K mol Ce} \approx 0.1R \ln 2$. This small entropy may imply that the FIM transition is associated with the ordering of Ce_{III} with the small moment of $0.1 \mu_B$.

The magnetic nature of the FIM transition is indicated by a small kink in the magnetization $M(T)$ at $B\parallel c = 2$ and 8 T as shown in Fig. 4(a). At 4 and 6 T, $M(T)$ exhibits no distinct anomaly. These observations can be understood if the field dependence of T_M is very small, that is, $dT_M/dB \approx 0$. Then, the Ehrenfest relation, $\Delta(\partial M/\partial T) = -(\partial T_M/\partial B)\Delta(C/T)$, gives $\Delta(\partial M/\partial T) = 0$. The temperature dependence of the capacitance of the magnetometer is shown in Fig. 4(b), where the data for two runs with and without a gradient field are plotted. At 6 T, a clear upturn is observed in both curves at around 0.65 K, which probably originates from a torque effect. When the temperature is lowered below T_M , the magnetic anisotropy in the FIM phase induces a torque in the crystal. This torque twists the capacitor plate on which the crystal is glued.¹⁷ In obtaining the magnetization value, the torque effect is eliminated by taking a difference between the capacitances with and without a gradient field. It is conjectured that the magnetic anisotropy arises from Ce_{III} spins having the magnetic easy axis perpendicular to the c axis.¹¹ At 0.5 T, on the other hand, no anomaly in both of $M(T)$ and capacitance curves suggests the persistence of the paramagnetic state down to 0.05 K.

Figure 5 shows the field dependence of the magnetization for $B\parallel c$ at temperatures below 0.45 K. A metamagnetic transition is seen at 0.3 T. The jump of magnetization of $0.37 \mu_B$ can be explained by assuming the spin-flip of Ce_I and Ce_{II} spins. The FIM transition manifests itself in a weak increase

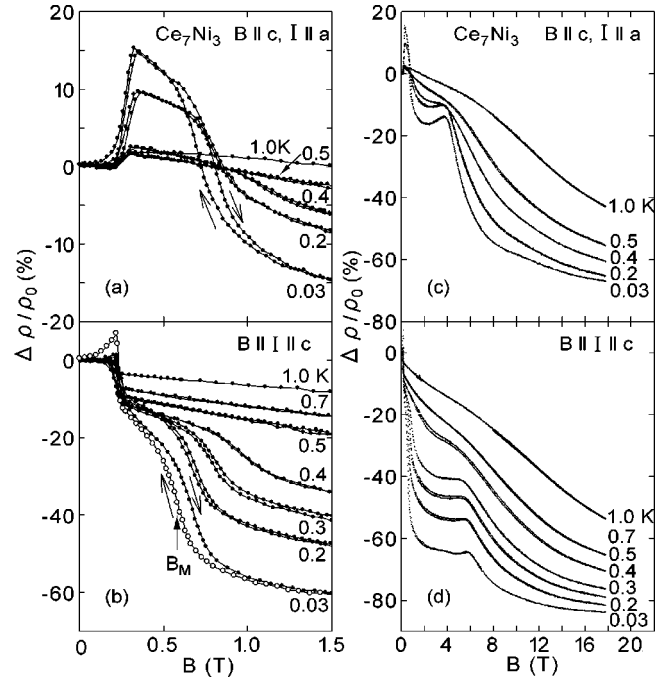


FIG. 6. Field ($B\parallel c$) dependence of magnetoresistance $\Delta\rho/\rho_0 = [\rho(B) - \rho(0)]/\rho(0)$ for the current directions $I\parallel a$ and $I\parallel c$. The field-induced magnetic transition field B_M was taken as the field of the inflection point of $\Delta\rho/\rho_0$.

of $M(B)$ at $B_M \approx 0.7 \text{ T}$. It is more clearly seen as a maximum in $\Delta M = M(0.05 \text{ K}) - M(0.45 \text{ K})$ in Fig. 5(b). The small jump of $0.004 \mu_B$ supports the conjecture that the Ce_{III} spins having the smallest moment partially align along the c axis. Furthermore, the hysteresis of $\Delta M(B)$ suggests that the transition from the paramagnetic state to the FIM state is of first order.

The magnetoresistance $\Delta\rho/\rho_0 = [\rho(B) - \rho(0)]/\rho(0)$ as a function of $B\parallel c$ is displayed in Fig. 6. The sharp anomaly in $\Delta\rho/\rho_0$ at $B = 0.2 \text{ T}$ is associated with the metamagnetic transition. On cooling below 0.4 K, the FIM transition manifests itself in the large decrease of $\Delta\rho/\rho_0$ at $B_M \approx 0.7 \text{ T}$ for both directions of measuring current $I\parallel a$ and $I\parallel c$. For $I\parallel c$ at the lowest temperature 0.03 K, the relative decrease of $\Delta\rho/\rho_0 \approx 40\%$ at $B \approx 0.7 \text{ T}$ is much larger than $\Delta\rho/\rho_0 \approx 12\%$ at $B = 0.2 \text{ T}$. This indicates that spin fluctuations remain in the field-induced paramagnetic phase but are largely quenched in the FIM phase. The hysteresis in $\Delta\rho/\rho_0$ found at around 0.7 T is consistent with that of $\Delta M(B)$ in Fig. 5(b). The maxima at 4–6 T suggest some sorts of phase transition in the FIM phase, while no anomaly in $M(B)$ has been found at that fields.

We now discuss the origin of the separation of the FIM phase from the SDW phase in the phase diagram shown in Fig. 1. To our knowledge, the field-induced magnetic phase appearing from a paramagnetic phase has been observed in four distinct systems; (a) spin-singlet ground-state systems, e.g., CsFeCl_3 ,²⁰ TlCuCl_3 ,²¹ and $\text{Ni}(\text{C}_5\text{H}_{14}\text{N}_2)_2\text{N}_3(\text{PF}_6)$,²² (b) the Ce-based superconductor CeCu_2Si_2 locating in the vicinity of quantum critical point,^{23–25} (c) quasi-two-dimensional organic conductors such as $(\text{TMTSF})_2\text{ClO}_4$,²⁶ and (d) geo-

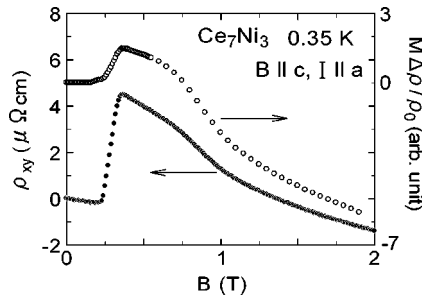


FIG. 7. Field ($B\parallel c$) dependence of Hall resistivity and $M\Delta\rho/\rho_0$ at 0.35 K, where M is the magnetization and $\Delta\rho/\rho_0$ is the relative magnetoresistance.

metrically frustrated magnets such as $\text{Gd}_3\text{Ga}_5\text{O}_{12}$.¹⁸ We consider the applicability of each scenario to Ce_7Ni_3 . First, the spin-singlet, ground-state system, which possesses a low-lying excited multiplet, can order magnetically at the level-crossing field if the exchange interaction is larger than the Zeeman energy. This scenario cannot be applied to Ce_7Ni_3 because the crystal-field ground state is a doublet according to the specific-heat data.¹⁰ Second, the origin of the FIM phase in CeCu_2Si_2 is still vague to the best of our knowledge, and, therefore we do not consider it further.

Third, for the quasi-two-dimensional system, the field-induced SDW (FISDW) occurs when the Fermi-surface nesting is incomplete. The Landau quantization in the pockets formed as the result of the incomplete nesting causes a series of gaps to appear around the main SDW gap. The Landau-quantization-assisted FISDW is unlikely to occur in the three-dimensional system Ce_7Ni_3 . If the FISDW occurs, the magnetoresistance should become positive, and the absolute value of Hall resistivity should increase due to the gap formation at the Fermi level. For Ce_7Ni_3 , however, the magnetoresistance for both $I\parallel a$ and $I\parallel c$ is negative at the FIM transition as shown in Fig. 6. The absolute value of Hall resistivity ρ_{xy} does not increase with fields, but exhibits similar field dependence as that of $M\Delta\rho/\rho_0$, as shown in Fig. 7. This fact suggests that the anomalous Hall effect is dominant at the FIM transition in Ce_7Ni_3 .

Fourth, for the geometrical frustrated system, a lack of magnetic order at low fields is caused by the strong spin fluctuations due to a geometrical frustration. Application of a magnetic field quenches the frustration, and leads to a transition to a magnetically ordered state. This scenario is possible for the FIM transition in Ce_7Ni_3 . By using the atomic positions of Ce_7Ni_3 determined at 7 K by powder neutron diffraction,¹¹ the average distances between one Ce atom and neighboring atoms in the coordination polyhedra defined by the Brunner-Schwarzenbach method²⁷ are 3.58, 3.58, and 3.54, respectively, for Ce_I , Ce_{II} , and Ce_{III} . These nearly equal distances for three sites suggest similar hybridization strength, and thus, similar size of magnetic moments for the three sites. Therefore, the strongest reduction of the ordered moment for Ce_{III} may result from not only the Kondo effect

but also a sort of frustration effect. In fact, strong reduction of ordered moments has been observed in geometrically frustrated heavy-fermion compounds, CePdAl and UNi_4B .^{28,29} For Ce_7Ni_3 , the geometrical frustration is expected in the quasiregular tetrahedron formed by Ce_I and Ce_{III} , as shown in the inset of Fig. 1. If the tetrahedron becomes a regular tetrahedron, the arrangement of magnetic atoms causes a strong geometrical frustration effect. Because the Ce_I - Ce_{III} distances in the tetrahedron are almost equal within a difference less than 4%,¹¹ a frustration effect should exist on Ce_I and Ce_{III} . In fact, a spin-glass transition due to the frustration is found in the isostructural compound Ce_7Ru_3 , of which the difference in interatomic distances is about 2%.⁹ In the tetrahedron, the three Ce_{III} atoms form a regular triangle, but the triangle made of one Ce_I and two Ce_{III} is slightly distorted. Therefore, the frustration effect on Ce_{III} should be larger than that on Ce_I . This may manifest itself in the smaller moments of Ce_{III} than that of Ce_I . The small anomalies in the specific heat and magnetization associated with the FIM transition could be explained by the rearrangement of Ce_{III} moments. The spin fluctuation due to the frustration prevents the magnetic moment of Ce_{III} from ordering in the field range $0.3 < B < 0.7$ T. Recently, fluctuating local fields have been observed in the external field above 0.3 T by muon-spin-rotation spectroscopy.³⁰ Beyond 0.7 T, however, Ce_{III} moments may be partially aligned along the c axis by the exchange fields produced by the field-induced ferromagnetic moments of Ce_I and Ce_{III} . In order to determine the magnetic structure of the FIM phase, a neutron diffraction study in magnetic fields is now in progress.

In summary, we have determined the B - T phase diagram of the heavy-fermion antiferromagnet Ce_7Ni_3 using the single-crystalline sample. A field-induced magnetic phase has been found for $B\parallel c > 0.7$ T and $T < 0.5$ K, which is separated from the SDW phase in the region $B\parallel c < 0.3$ T. Combination of the results of specific heat and magnetization suggests that the rearrangement of the Ce_{III} moments is responsible for the field-induced magnetic order. We attribute the separation from the low-field SDW phase to large spin fluctuations on Ce_{III} , which originate from a geometrical frustration in the quasiregular tetrahedron made of Ce_I and Ce_{III} atoms in Ce_7Ni_3 .

ACKNOWLEDGMENTS

We acknowledge H. Kadowaki for helpful discussions. Specific-heat measurements were carried out at the Cryogenic Center, Hiroshima University. Resistivity and magnetization measurements under magnetic fields were performed as joint research at the National Institute for Materials Science and ISSP of the University of Tokyo, respectively. This work was supported by the COE Research (Grant No. 13CE2002) in a Grant-in-Aid from the Ministry of Education, Culture, Sports, Science and Technology of Japan.

*Email address: kumeo@sci.hiroshima-u.ac.jp

[†]Present address: National Research Laboratory for Material Science, KBSI, 52 Yeoeun-dong, Yuseung-ku, Daejeon 305-333, South Korea.

¹A. P. Ramirez, in *Handbook of Magnetic Materials*, edited by K. H. J. Buschow (Elsevier Science B.V., Amsterdam, 2001), Vol. 13, p. 426.

²M. Shiga, K. Fujisawa, and H. Wada, *J. Phys. Soc. Jpn.* **62**, 1329 (1993).

³C. Urano, M. Nohara, S. Kondo, F. Sakai, H. Takagi, T. Shiraki, and T. Okubo, *Phys. Rev. Lett.* **85**, 1052 (2000).

⁴M. Hanawa, Y. Muraoka, T. Tayama, T. Sakakibara, J. Yamaura, and Z. Hiroi, *Phys. Rev. Lett.* **87**, 187001 (2001).

⁵A. Donni, H. Kitazawa, P. Fischer, J. Tang, M. Kohgi, Y. Endoh, and Y. Morii, *J. Phys.: Condens. Matter* **7**, 1663 (1995).

⁶Y. Isikawa, T. Mizushima, N. Fukushima, T. Kuwai, J. Sakurai, and H. Kitazawa, *J. Phys. Soc. Jpn.* **65**, 117 (1996).

⁷R.B. Roof, Jr., A.C. Larson, and D.T. Cromer, *Acta Crystallogr.* **14**, 1084 (1961).

⁸D. Gignoux and D. Schmitt, in *Handbook on the Physics and Chemistry of Rare Earths*, edited by K. A. Gschneidner, Jr. and L. Eyring (Elsevier Science B. V., Amsterdam, 1995), Vol. 20, p. 293.

⁹O. Trovarelli, J.G. Sereni, and J.P. Kappler, *J. Low Temp. Phys.* **108**, 53 (1997).

¹⁰K. Umeo, T. Takabatake, N. Sato, T. Komatsubara, K. Oda, and K. Kindo, *J. Phys. Soc. Jpn.* **66**, 2133 (1997).

¹¹H. Kadowaki, K. Motoya, T. Kawasaki, T. Osakabe, H. Okumura, K. Kakurai, K. Umeo, and T. Takabatake, *J. Phys. Soc. Jpn.* **69**, 2269 (2000).

¹²K. Umeo, H. Kadomatsu, and T. Takabatake, *J. Phys.: Condens. Matter* **8**, 9743 (1996).

¹³K. Umeo, H. Kadomatsu, and T. Takabatake, *Phys. Rev. B* **55**, R692 (1997).

¹⁴K. Umeo, T. Takabatake, H. Ohmoto, T. Pietrus, H.v. Löhneysen,

K. Koyama, S. Hane, and T. Goto, *Phys. Rev. B* **58**, 12 095 (1998).

¹⁵J.G. Sereni, O. Trovarelli, J.P. Kappler, C. Paschke, T. Trappmann, and H.v. Löhneysen, *Physica B* **199-200**, 567 (1994).

¹⁶J.S. Kim, K. Heuser, and G.R. Stewart, *Solid State Commun.* **108**, 261 (1998).

¹⁷T. Sakakibara, H. Mitamura, T. Tayama, and H. Amitsuka, *Jpn. J. Appl. Phys.* **33**, 5067 (1994).

¹⁸P. Schiffer, A.P. Ramirez, D.A. Huse, and A.J. Valentino, *Phys. Rev. Lett.* **73**, 2500 (1994).

¹⁹E. Cattaneo, *Z. Phys. B: Condens. Matter* **64**, 305 (1986).

²⁰M. Chiba, S. Ueda, T. Yanagimoto, M. Toda, and T. Goto, *Physica B* **284-288**, 1529 (2000).

²¹T. Nikuni, M. Oshikawa, A. Oosawa, and H. Tanaka, *Phys. Rev. Lett.* **84**, 5868 (2000).

²²E.L. Carlin, and L.J. De Jongh, *Chem. Rev.* **86**, 659 (1986).

²³P. Gegenwart, C. Langhammer, C. Geibel, R. Helfrich, M. Lang, G. Sparn, F. Steglich, R. Horn, L. Donnevert, A. Link, and W. Assmus, *Phys. Rev. Lett.* **81**, 1501 (1998).

²⁴G. Bruls, B. Wolf, D. Finsterbusch, P. Thalmeier, I. Kouroudis, W. Sun, W. Assmus, B. Lüthi, M. Lang, K. Gloos, F. Steglich, and R. Modler, *Phys. Rev. Lett.* **72**, 1754 (1994).

²⁵F. Steglich, P. Gegenwart, C. Geibel, P. Hinze, M. Lang, C. Langhammer, G. Sparn, and O. Trovarelli, *Physica B* **280**, 349 (2000).

²⁶M.J. Naughton, R.V. Chamberlin, X. Yan, S.-Y. Hsu, L.Y. Chiang, M.Y. Azbel, and P.M. Chaikin, *Phys. Rev. Lett.* **61**, 621 (1988).

²⁷G.O. Brunner and D. Schwarzenbach, *Z. Kristallogr.* **133**, 127 (1971).

²⁸M.D. Núñez-Regueiro, C. Lacroix, and B. Canals, *Physica C* **282-287**, 1885 (1997).

²⁹C. Lacroix, B. Canals, and M.D. Núñez-Regueiro, *Phys. Rev. Lett.* **77**, 5126 (1996).

³⁰A. Schenck, F. N. Gygax, D. Andreica, K. Umeo, and T. Takabatake, *Physica B* **326**, 394 (2003).